

**Electronic Supplementary Information**

**Triazole-bearing Calixpyrroles: Strong Halide Binding Affinities through Multiple N-H and C-H Hydrogen Bondings**

**Hyeongcheol Kim, Kyeong-Im Hong, Jeong Heon Lee, Philjae Kang, Moon-Gun Choi, and Woo-Dong Jang\***

Department of Chemistry, Yonsei University

50 Yonsei-ro, Seodaemun-gu, Seoul 03722, Korea

**Contents**

- 1. Materials and measurements**
- 2. Synthesis and characterization**
- 3. X-ray crystallographic data**
- 4. NMR titrations and binding study of calix[4]pyrroles**
- 5. DFT calculation for the optimized structures of TCPs binding with halide ion**
- 6. Reference**

## 1. Materials and measurements

All commercially available reagents were reagent grade and used without further purification. Dichloromethane (DCM) and tetrahydrofuran (THF) were freshly distilled before each use. All anions used for NMR experiment were in the form of the tetrabutylammonium salt.  $^1\text{H}$ ,  $^{13}\text{C}$  NMR spectra were recorded using a Bruker DPX 400 (400 MHz) spectrometer at 25 °C in  $\text{CDCl}_3$ ,  $\text{CD}_3\text{CN}$  or  $(\text{CD}_3)_2\text{SO}$ . UV/Vis absorption spectra were recorded on a JASCO model V-660 spectrometer. MALDI-TOF-MS was performed on a Bruker Daltonics LRF20 with dithranol as the matrix.

## 2. Synthesis and characterization

**1-azidopropan-2-one (1):** Chloroacetone (4.8 mL, 60 mmol) and sodium azide (6.0 g, 100 mmol) were added in acetone (150 mL) and the reaction mixture was stirred for 23 h at room temperature. After the solvent was removed, the residue was extracted with  $\text{CH}_2\text{Cl}_2/\text{H}_2\text{O}$ , and the organic layer was concentrated. The residue was purified by column chromatography eluting with 11% EA/HX to give **3** (6.1 g, 62%).<sup>1</sup>  $^1\text{H}$  NMR (400MHz,  $\text{CDCl}_3$ , 25 °C)  $\delta$  (ppm): 3.96 (s, 2 H), 2.20 (s, 3 H)

**1-(1-phenyl-1H-1,2,3-triazol-4-yl)ethenone (2):** Azidoacetone (2.50 g, 25.2 mmol) and phenylacetylene (3.10 g, 30.3 mmol) were added in anhydrous THF (180 mL).  $\text{CuSO}_4 \cdot 5\text{H}_2\text{O}$  (4.02 g, 25.2 mmol) and sodium ascorbate (4.99 g, 25.2 mmol) dissolved in  $\text{H}_2\text{O}$  were added, and the reaction mixture was refluxed for 12 h at 60 °C. After filtration, the solution was extracted with  $\text{NaCl(aq)}/\text{CH}_2\text{Cl}_2$ , and the organic layer was concentrated. The residue was purified by column chromatography eluting with 3% MeOH/ $\text{CH}_2\text{Cl}_2$  to give **4** (3.95 g, 78%).  $^1\text{H}$  NMR (400MHz,  $\text{CDCl}_3$ , 25 °C)  $\delta$  (ppm): 7.86 – 7.83 (m, 2 H), 7.84 (s, 1 H), 7.46 – 7.42 (m, 2 H), 7.37 – 7.33 (m, 1 H), 5.25 (s, 2 H), 2.28 (s, 3 H).

**Phenyltriazole dipyrrole (3):** Trifluoroacetic acid (1.5 mL) was added dropwise to **4** (2.0 g, 9.94 mmol) in pyrrole (50 mL, excess), and the reaction mixture was refluxed for 7 h at 50 °C. Triethylamine (1.5 mL) was added to a solution and the solution was concentrated under high vacuum to remove pyrrole. After extraction with  $\text{NaCl(aq)}/\text{CH}_2\text{Cl}_2$ , the residue was purified by column chromatography eluting with 3% THF/ $\text{CH}_2\text{Cl}_2$ , 10% EA/ $\text{CH}_2\text{Cl}_2$  to give **5** (2.0 g, 63%).  $^1\text{H}$  NMR (400MHz,  $\text{CDCl}_3$ , 25 °C)  $\delta$  (ppm): 8.14 (broad s, 2 H), 7.68 – 7.65 (m, 2 H), 7.40 – 7.36 (m, 2 H), 7.32 – 7.28 (m, 1 H), 6.73 – 6.71 (m, 2 H), 6.62 (s, 1 H), 6.24 – 6.22 (m, 2 H), 6.18 – 6.17 (m, 2 H), 4.88 (s, 2 H), 1.65 (s, 3 H).

**Phenyltriazole calix[4]pyrrole (TCP):** BF<sub>3</sub>.OEt<sub>2</sub> (1.5 mL) was added dropwise to **5** (2.0g, 6.3 mmol) in acetone (500 mL, excess), and the reaction mixture was stirred for 4 h at 25 °C. Triethylamine (1.5 mL) was added to a solution and the reaction mixture was diluted with CH<sub>2</sub>Cl<sub>2</sub>, extracted with H<sub>2</sub>O, and concentrated. The residue was purified by column chromatography eluting with 15% EA/CH<sub>2</sub>Cl<sub>2</sub> to give pure both *trans*-TCP and *cis*-TCP (400 mg, overall yield 18%).

#### *Trans*-TCP

<sup>1</sup>H NMR (400MHz, (CD<sub>3</sub>)<sub>2</sub>SO, 25 °C) δ (ppm): 9.87 (broad s, 4 H), 7.62 – 7.61 (d, *J* = 4 Hz, 4 H), 7.45 – 7.41 (t, *J* = 16 Hz, 4 H), 7.33 – 7.29 (t, *J* = 16 Hz, 2 H), 7.02 (s, 2 H), 5.83 – 5.82 (m, 8 H), 5.03 (s, 4 H), 1.65 (s, 12 H), 1.48 (s, 6 H); <sup>13</sup>C NMR (100 MHz, CDCl<sub>3</sub>, 25 °C) δ (ppm): 147.43, 139.94, 133.46, 130.98, 129.14, 128.35, 125.87, 120.71, 120.67, 106.22, 104.42, 59.07, 41.07, 35.84, 30.19, 25.60; MALDI-TOF-MS *m/z* : cald. for C<sub>44</sub>H<sub>46</sub>N<sub>10</sub>: 714.90 [M+H]<sup>+</sup>; found : 715.2.

#### *Cis*-TCP

<sup>1</sup>H NMR (400MHz, (CD<sub>3</sub>)<sub>2</sub>SO, 25 °C) δ (ppm): 9.51 (broad s, 4 H), 7.66 – 7.63 (m, 4 H), 7.44 – 7.40 (m, 4 H), 7.33 – 7.29 (m, 2 H), 7.06 (s, 2 H), 5.89 – 5.88 (t, *J* = 4 Hz, 4 H), 5.81 – 5.80 (t, *J* = 4 Hz, 4 H), 4.91 (s, 4 H), 1.56 (s, 6 H), 1.53 (s, 6 H), 1.51 (s, 6 H); <sup>13</sup>C NMR (100 MHz, (CD<sub>3</sub>)<sub>2</sub>SO, 25 °C) δ (ppm): 145.49, 139.55, 133.68, 130.72, 129.02, 127.89, 124.92, 121.33, 104.38, 102.55, 58.35, 34.73, 30.10, 28.27, 24.32; MALDI-TOF-MS *m/z* : cald. for C<sub>44</sub>H<sub>46</sub>N<sub>10</sub>: 714.90 [M+Na]<sup>+</sup>; found : 737.5.

**Octamethyl calix[4]pyrrole (OMCP):** Acetone(2.2 mL, 30 mmol) and pyrrole(1.97 mL, 28.5 mmol) were dissolved in dichloromethane(200 mL) and trifluoroacetic acid (1.1 mL) was added dropwise to the solution. The reaction mixture was stirred for 13 h at RT. NaHCO<sub>3</sub> was added to a solution and the solution was concentrated. After that, the residue was extracted with CH<sub>2</sub>Cl<sub>2</sub>/H<sub>2</sub>O, and the organic layer was concentrated. The residue was purified by column chromatography eluting with 50% DCM/HX to give **2** (462 mg, 15%). <sup>1</sup>H NMR (400MHz, CDCl<sub>3</sub>, 25 °C) δ (ppm): 6.98 (broad s, 4 H), 5.90 – 5.89 (d, *J* = 4 Hz, 8 H), 1.51 (s, 24 H).

### 3. X-ray crystallographic data

#### *Trans*-TCP

#### Single crystal growing

*Trans*-TCP was dissolved completely in chloroform&acetonitrile and the solution was filtrated with celite. Afterward, the filtrated solution was vapor-diffused with diethyl ether at room temperature to obtain white single crystals suitable for the SC-XRD.

#### Data collection

The diffraction data from colorless crystals of *trans*-TCP ( $0.126 \times 0.035 \times 0.022 \text{ mm}^3$ ) mounted on a MiTeGen MicroMount© were collected at 100 on a ADSC Quantum 210 CCD diffractometer with synchrotron radiation (0.63 Å) at Supramolecular Crystallography 2D, Pohang Accelerator Laboratory (PAL), Pohang, Korea. The ADSC Q210 ADX program was used for data collection (detector distance is 63 mm, omega scan;  $\Delta\omega = 1^\circ$ , exposure time is 1 sec/frame for *trans*-TCP and HKL3000sm (Ver. 703r) was used for cell refinement, reduction and absorption correction. The crystal structures of *trans*-TCP were solved by the direct method with SHELX-XT (Ver. 2014/5) and refined by full-matrix least-squares calculations with the SHELX-XL (Ver. 2016/4) program package.<sup>2-5</sup>

#### Structure solution and refinement

The systematic absences in the diffraction data were uniquely consistent for the monoclinic space group  $P2_1/n$  that yielded chemically reasonable and computationally stable results of refinement.<sup>6</sup>

A successful solution by the direct methods provided most non-hydrogen atoms from the *E*-map. The remaining non-hydrogen atoms were located in an alternating series of least-squares cycles and difference Fourier maps. All non-hydrogen atoms were refined with anisotropic displacement coefficients. All hydrogen atoms were included in the structure factor calculation at idealized positions and allowed to ride on the neighboring atoms with relative isotropic displacement coefficients.

The final least-squares refinement of 493 parameters against 15928 data resulted in residuals *R* (based on  $F^2$  for  $I \geq 2\sigma$ ) and *wR* (based on  $F^2$  for all data) of 0.0533 and 0.1745, respectively. The final difference Fourier map was featureless.

#### Summary

Crystal Data for  $C_{44}H_{46}N_{10}$  ( $M = 714.91 \text{ g/mol}$ ): monoclinic, space group  $P2_1/c$  (no. 14),  $a = 12.546(3) \text{ \AA}$ ,  $b = 27.351(6) \text{ \AA}$ ,  $c = 11.169(2) \text{ \AA}$ ,  $\beta = 93.95(3)^\circ$ ,  $V = 3823.5(13) \text{ \AA}^3$ ,  $Z = 4$ ,  $T = 100.0 \text{ K}$ ,  $\mu(?) = 0.060 \text{ mm}^{-1}$ ,  $D_{calc} =$

1.242 g/cm<sup>3</sup>, 29162 reflections measured (3.498° ≤ 2Θ ≤ 66.65°), 15928 unique ( $R_{\text{int}} = 0.0432$ ,  $R_{\text{sigma}} = 0.0625$ ) which were used in all calculations. The final  $R_1$  was 0.0533 ( $I > 2\sigma(I)$ ) and  $wR_2$  was 0.1745 (all data).

**Table S1.** Crystal data and structure refinement for *trans*-TCP.

Identification code	calixpyrrole_trans
Empirical formula	C <sub>44</sub> H <sub>46</sub> N <sub>10</sub>
Formula weight	714.91
Temperature/K	100
Crystal system	monoclinic
Space group	P2 <sub>1</sub> /c
a/Å	12.546(3)
b/Å	27.351(6)
c/Å	11.169(2)
α/°	90
β/°	93.95(3)
γ/°	90
Volume/Å <sup>3</sup>	3823.5(13)
Z	4
ρ <sub>calc</sub> /g/cm <sup>3</sup>	1.242
μ/mm <sup>-1</sup>	0.060
F(000)	1520.0
Crystal size/mm <sup>3</sup>	0.126 × 0.035 × 0.022
Radiation	synchrotron (λ = 0.630)
2Θ range for data collection/°	3.49 to 66.65
Index ranges	-19 ≤ h ≤ 19, -42 ≤ k ≤ 42, -15 ≤ l ≤ 15
Reflections collected	29162
Independent reflections	15928 [ $R_{\text{int}} = 0.0432$ , $R_{\text{sigma}} = 0.0625$ ]
Data/restraints/parameters	15928/12/493
Goodness-of-fit on F <sup>2</sup>	1.034
Final R indexes [ $I \geq 2\sigma(I)$ ]	$R_1 = 0.053$ , $wR_2 = 0.150$
Final R indexes [all data]	$R_1 = 0.082$ , $wR_2 = 0.174$
Largest diff. peak/hole / e Å <sup>-3</sup>	0.65/-0.66

## *Cis*-TCP

### Single crystal growing

*Cis*-TCP was dissolved completely in acetonitrile by increasing temperature up to 70 °C. Afterward, the solution was cooled down so slowly to obtain yellow single crystals suitable for the SC-XRD.

### Data collection

A crystal with approximate dimensions  $0.13 \times 0.04 \times 0.025$  mm<sup>3</sup> was selected under oil under ambient conditions and attached to the tip of a MiTeGen MicroMount©. The crystal was mounted and centered in the X-ray beam by using a video camera.

The crystal evaluation and data collection were performed on a Bruker D8 Venture diffractometer with Mo K<sub>α</sub> ( $\lambda = 0.71073$  Å) radiation and the diffractometer to crystal distance of 4.00 cm.

The initial cell constants were obtained from three series of  $\omega$  scans at different starting angles. Each series consisted of 12 frames collected at intervals of 0.5° in  $\omega$  range about  $\omega$  with the exposure time of 3 seconds per frame. The reflections were successfully indexed by an automated indexing routine built in the APEXII program. The final cell constants were calculated from a set of 9943 strong reflections from the actual data collection.

The data were collected by using the full sphere data collection routine to survey the reciprocal space to the extent of a full sphere to a resolution of 0.81 Å. A total of 76957 were harvested by collecting 3 set of frames with 0.5° scans in  $\omega$  and  $\phi$  with an exposure time 5 sec per frame. These highly redundant datasets were corrected for Lorentz and polarization effects. The absorption correction was based on fitting a function to the empirical transmission surface as sampled by multiple equivalent measurements.<sup>7</sup>

### Structure solution and refinement

The systematic absences in the diffraction data were uniquely consistent for monoclinic, space group P2<sub>1</sub>/n that yielded chemically reasonable and computationally stable results of refinement.<sup>6, 8</sup>

A successful solution by the direct methods provided most non-hydrogen atoms from the *E*-map. The remaining non-hydrogen atoms were located in an alternating series of least-squares cycles and difference Fourier maps. All non-hydrogen atoms were refined with anisotropic displacement coefficients. All hydrogen atoms were included in the structure factor calculation at idealized positions and were allowed to ride on the neighboring atoms with relative isotropic displacement coefficients.

The final least-squares refinement of 494 parameters against 8195 data resulted in residuals *R* (based on  $F^2$  for  $I \geq 2\sigma$ ) and *wR* (based on  $F^2$  for all data) of 0.0714 and 0.1766 respectively. The final difference Fourier map was featureless.

## Summary

Crystal Data for  $C_{44}H_{45.9775}N_{10}$  ( $M=714.88$  g/mol): monoclinic, space group  $P2_1/n$  (no. 14),  $a = 12.5203(6)$  Å,  $b = 19.8938(10)$  Å,  $c = 16.9880(9)$  Å,  $\beta = 102.163(2)^\circ$ ,  $V = 4136.3(4)$  Å<sup>3</sup>,  $Z = 4$ ,  $T = 304.6$  K,  $\mu(\text{MoK}\alpha) = 0.071$  mm<sup>-1</sup>,  $D_{\text{calc}} = 1.148$  g/cm<sup>3</sup>, 76957 reflections measured ( $4.532^\circ \leq 2\Theta \leq 52.204^\circ$ ), 8195 unique ( $R_{\text{int}} = 0.1014$ ,  $R_{\text{sigma}} = 0.0520$ ) which were used in all calculations. The final  $R_1$  was 0.0714 ( $I > 2\sigma(I)$ ) and  $wR_2$  was 0.1766 (all data).

**Table S2.** Crystal data and structure refinement for *cis*-TCP.

Identification code	calixpyrrole_cis
Empirical formula	$C_{44}H_{45.98}N_{10}$
Formula weight	714.88
Temperature/K	304
Crystal system	monoclinic
Space group	$P2_1/n$
$a/\text{Å}$	12.5203(6)
$b/\text{Å}$	19.8938(10)
$c/\text{Å}$	16.9880(9)
$\alpha/^\circ$	90
$\beta/^\circ$	102.163(2)
$\gamma/^\circ$	90
Volume/Å <sup>3</sup>	4136.3(4)
$Z$	4
$\rho_{\text{calc}}/\text{cm}^3$	1.148
$\mu/\text{mm}^{-1}$	0.071
$F(000)$	1520.0
Crystal size/mm <sup>3</sup>	$0.13 \times 0.04 \times 0.025$
Radiation	MoK $\alpha$ ( $\lambda = 0.71073$ )
$2\Theta$ range for data collection/ $^\circ$	4.53 to 52.20
Index ranges	$-15 \leq h \leq 13$ , $-24 \leq k \leq 24$ , $-20 \leq l \leq 20$
Reflections collected	76957
Independent reflections	8195 [ $R_{\text{int}} = 0.1014$ , $R_{\text{sigma}} = 0.0520$ ]
Data/restraints/parameters	8195/0/494
Goodness-of-fit on $F^2$	1.055
Final R indexes [ $I \geq 2\sigma(I)$ ]	$R_1 = 0.071$ , $wR_2 = 0.155$
Final R indexes [all data]	$R_1 = 0.120$ , $wR_2 = 0.176$
Largest diff. peak/hole / $e \text{ Å}^{-3}$	0.41/-0.30

#### 4. Binding study of calix[4]pyrroles through NMR titration

All binding studies of calix[4]pyrroles for halide ions were examined by using  $^1\text{H}$  NMR spectroscopy in  $\text{CD}_3\text{CN}/\text{CDCl}_3(1/9, \text{v/v})$  solvent condition.

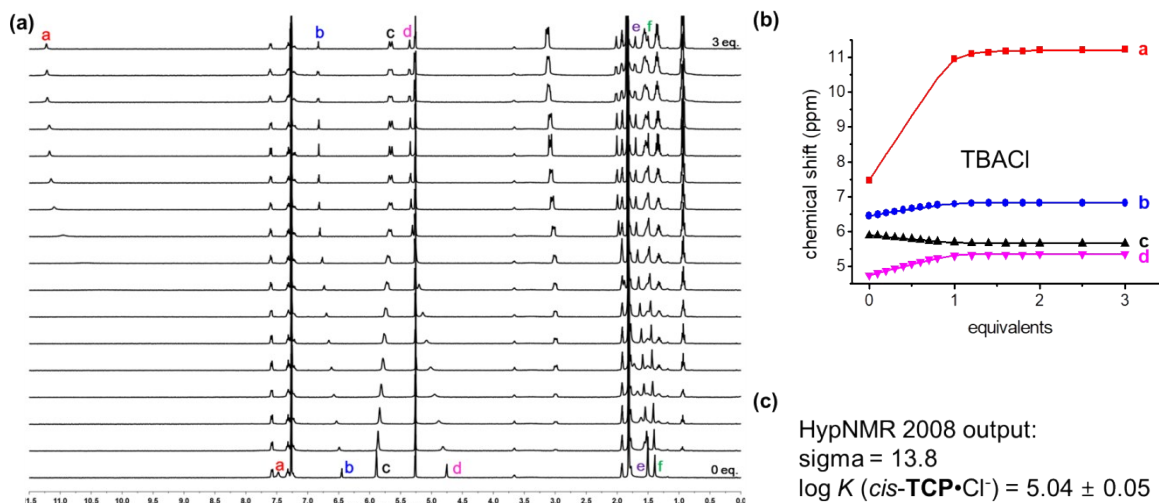


**Figure S1.** (a) Stacked NMR spectra of *cis*-TCP with TBACl, (b) chemical shift change of *cis*-TCP's protons upon addition of TBACl, (c) binding constant calculated from HypNMR.

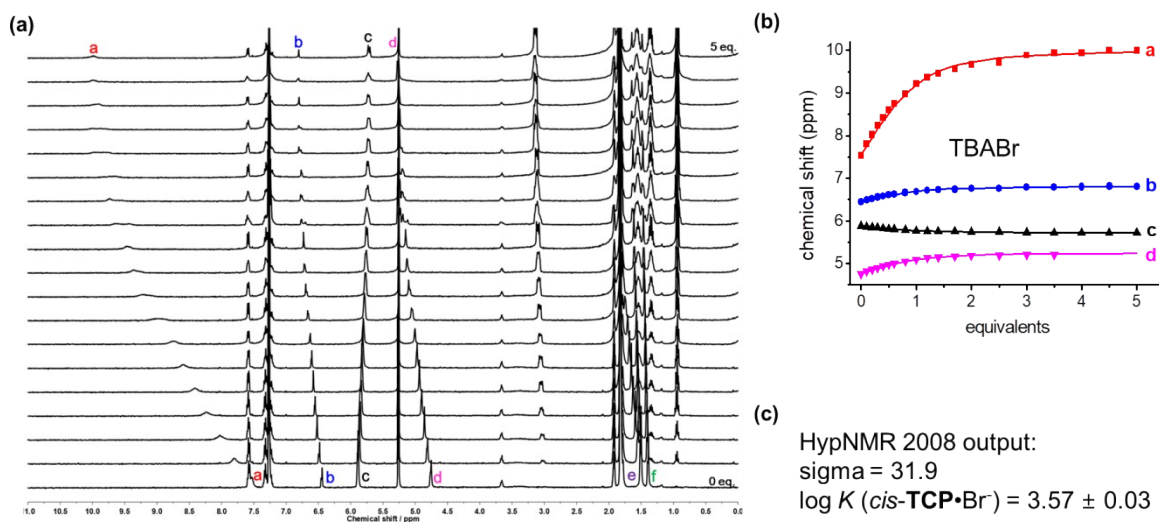


**Figure S2.** (a) Stacked NMR spectra of *cis*-TCP with TBABr, (b) chemical shift change of *cis*-TCP's protons upon addition of TBABr, (c) binding constant calculated from HypNMR.

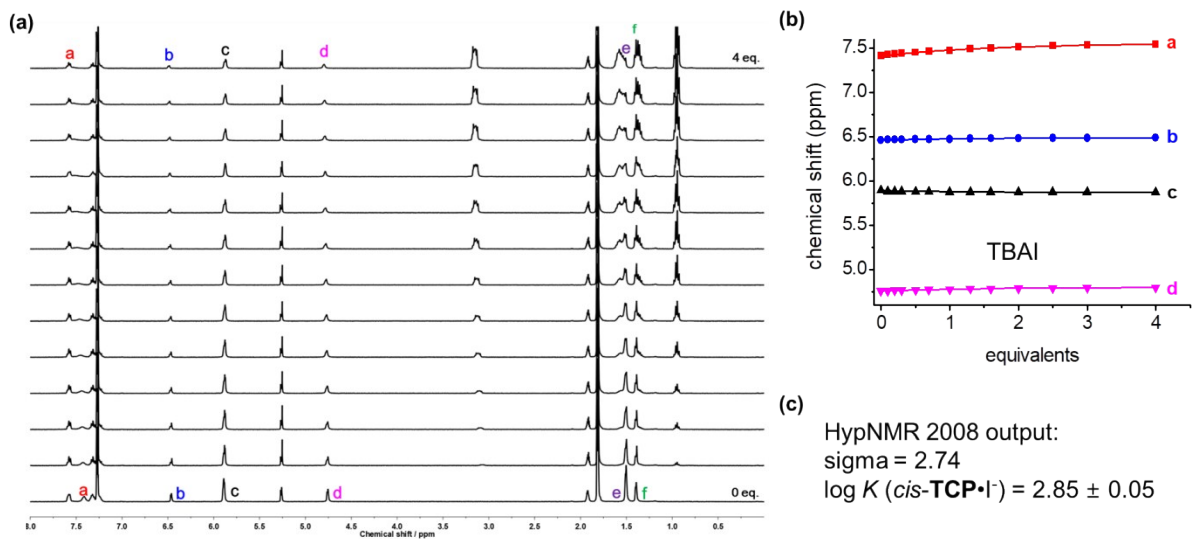


**Figure S3.** (a) Stacked NMR spectra of *cis*-TCP with TBAI, (b) chemical shift change of *cis*-TCP's protons upon addition of TBAI, (c) binding constant calculated from HypNMR.

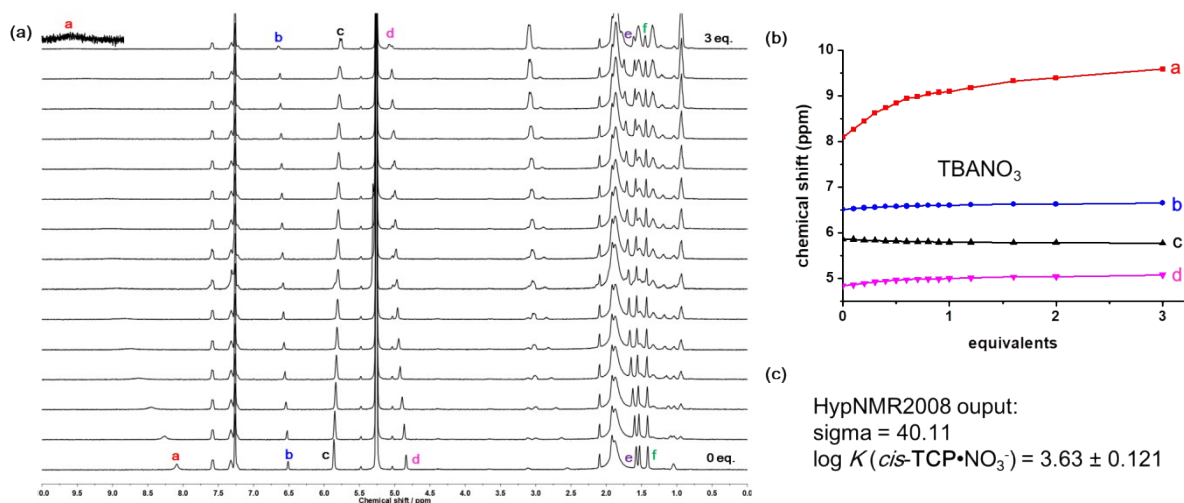


**Figure S4.** (a) Stacked NMR spectra of *cis*-TCP with TBANO<sub>3</sub>, (b) chemical shift change of *cis*-TCP's protons upon addition of TBANO<sub>3</sub>, (c) binding constant calculated from HypNMR.

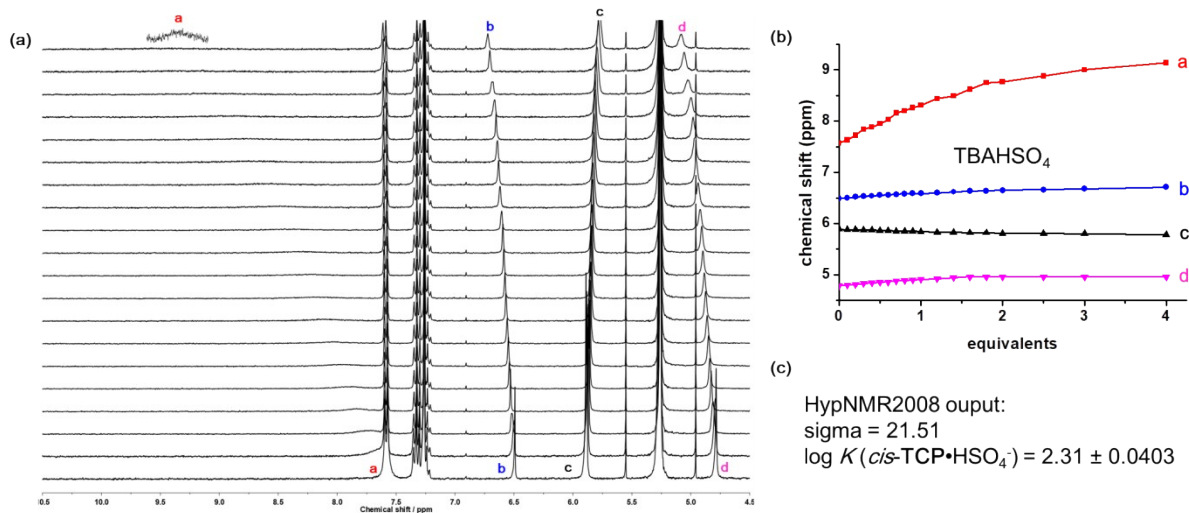


**Figure S5.** (a) Stacked NMR spectra of *cis*-TCP with TBAHSO<sub>4</sub>, (b) chemical shift change of *cis*-TCP's protons upon addition of TBAHSO<sub>4</sub>, (c) binding constant calculated from HypNMR.

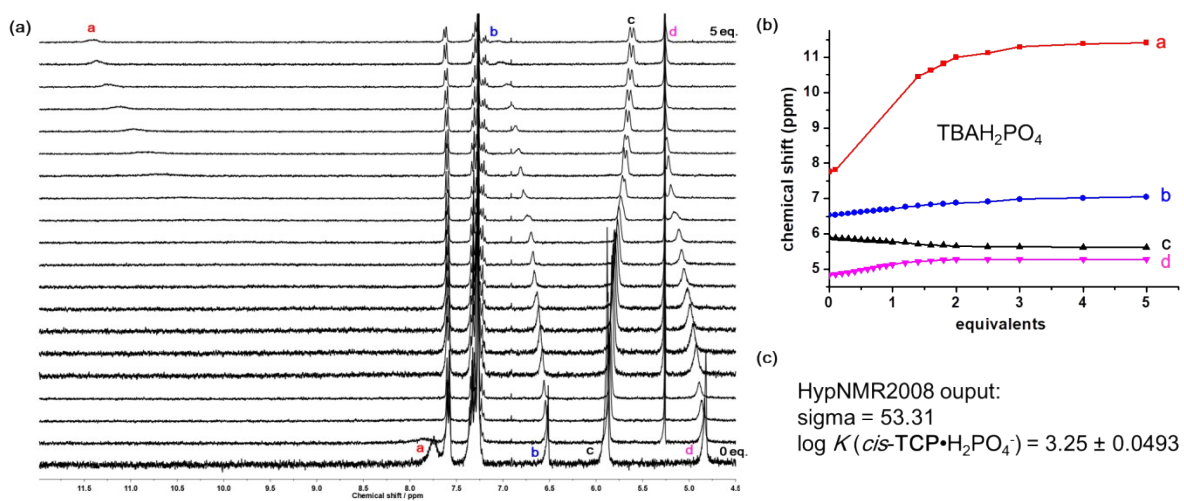


**Figure S6.** (a) Stacked NMR spectra of *cis*-TCP with TBAH<sub>2</sub>PO<sub>4</sub>, (b) chemical shift change of *cis*-TCP's protons upon addition of TBAH<sub>2</sub>PO<sub>4</sub>, (c) binding constant calculated from HypNMR.

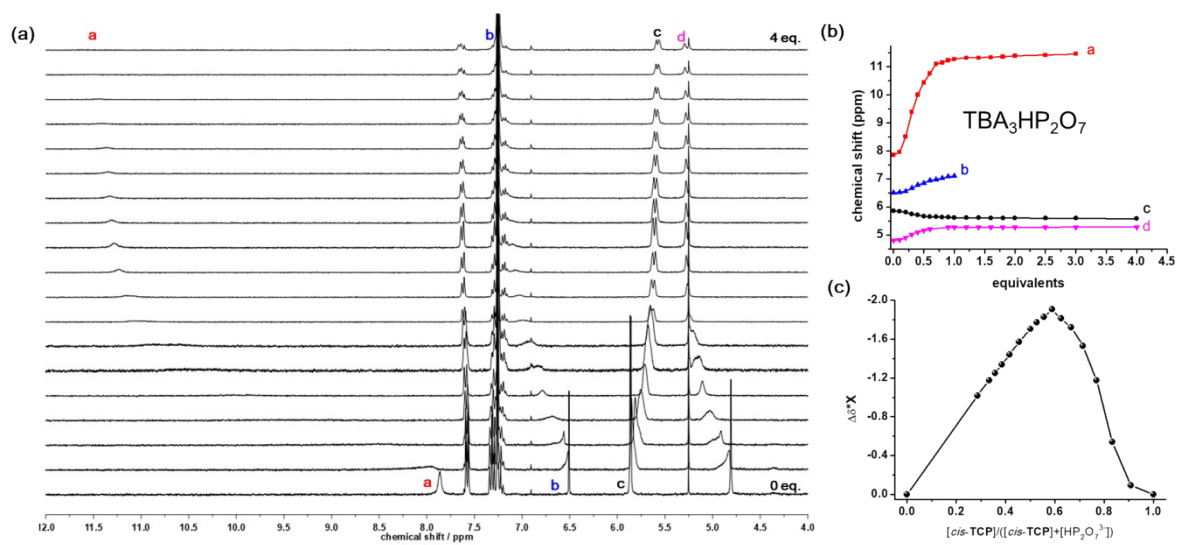


**Figure S7.** (a) Stacked NMR spectra of *cis*-TCP with TBA<sub>3</sub>HP<sub>2</sub>O<sub>7</sub>, (b) chemical shift change of *cis*-TCP's protons upon addition of TBA<sub>3</sub>HP<sub>2</sub>O<sub>7</sub>, (c) Job's plot for the addition of HP<sub>2</sub>O<sub>7</sub><sup>3-</sup> ions to *cis*-TCP.

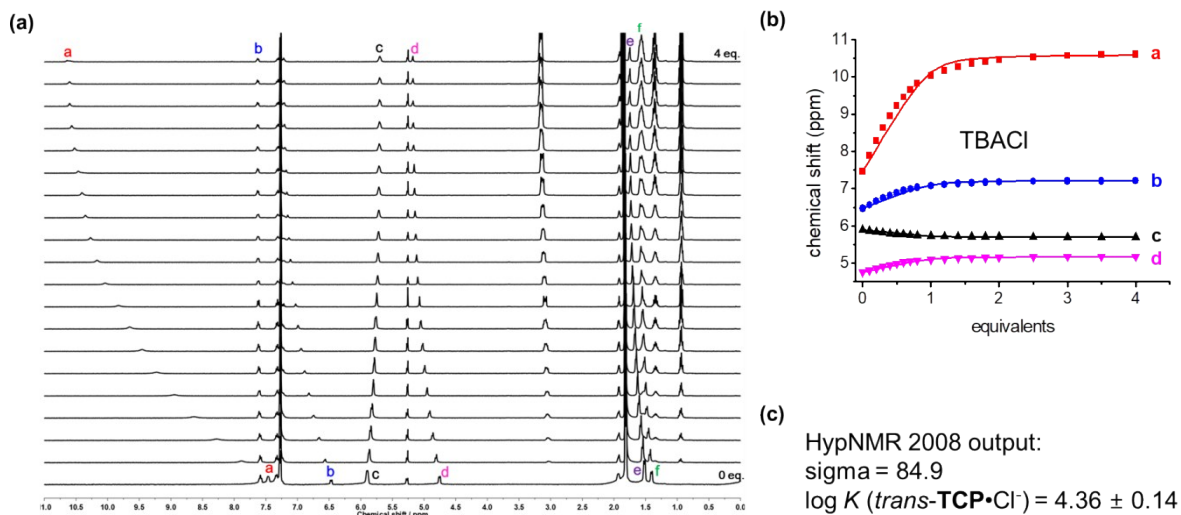


**Figure S8.** (a) Stacked NMR spectra of *trans*-TCP with TBACl, (b) chemical shift change of *trans*-TCP's protons upon addition of TBACl, (c) binding constant calculated from HypNMR.

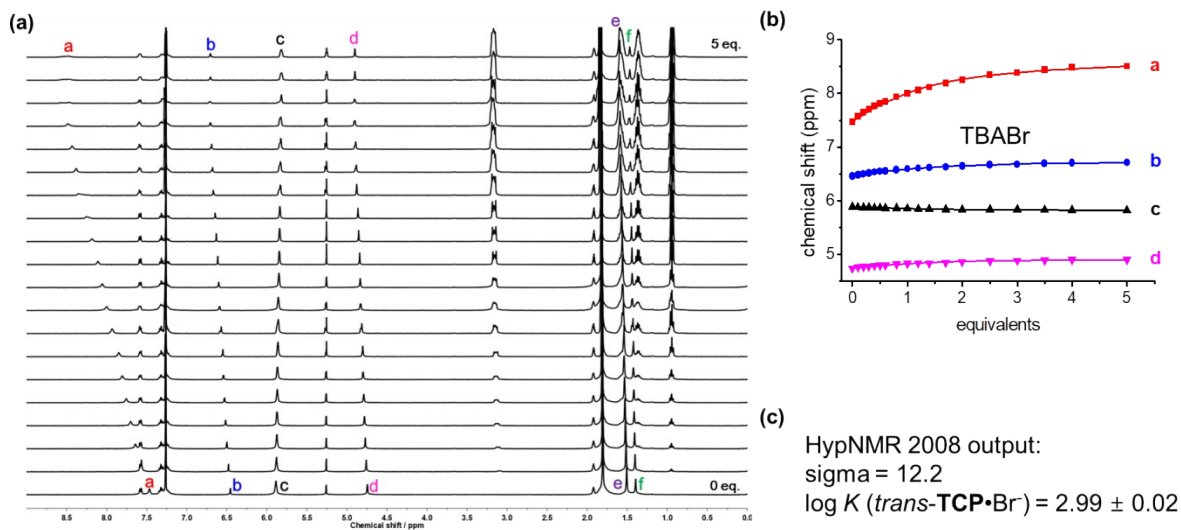


**Figure S9.** (a) Stacked NMR spectra of *trans*-TCP with TBABr, (b) chemical shift change of *trans*-TCP's protons upon addition of TBABr, (c) binding constant calculated from HypNMR.

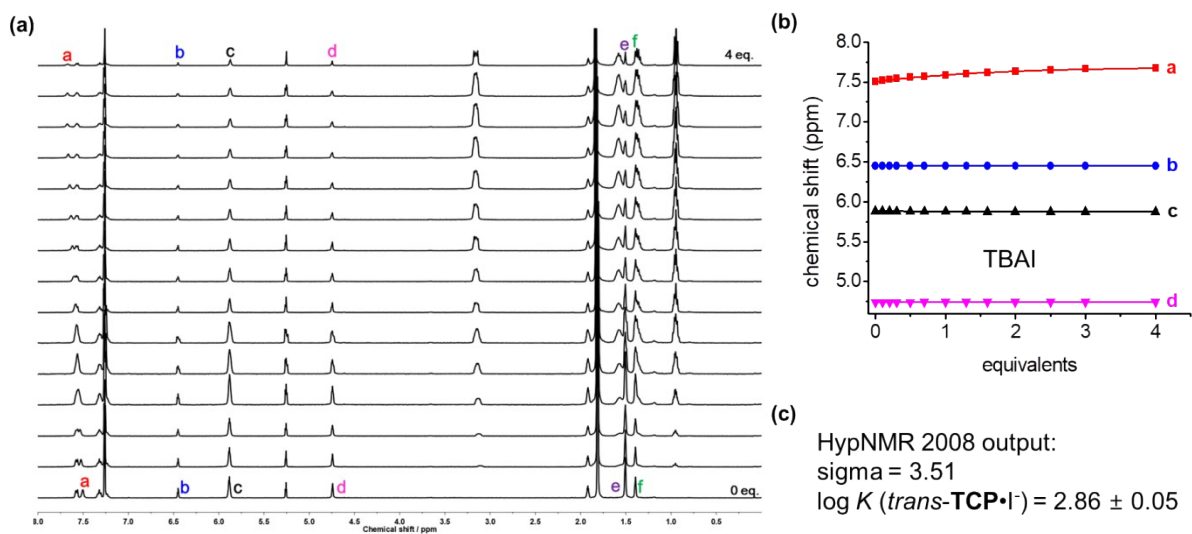


**Figure S10.** (a) Stacked NMR spectra of *trans*-TCP with TBAI, (b) chemical shift change of *trans*-TCP's protons upon addition of TBAI, (c) binding constant calculated from HypNMR.

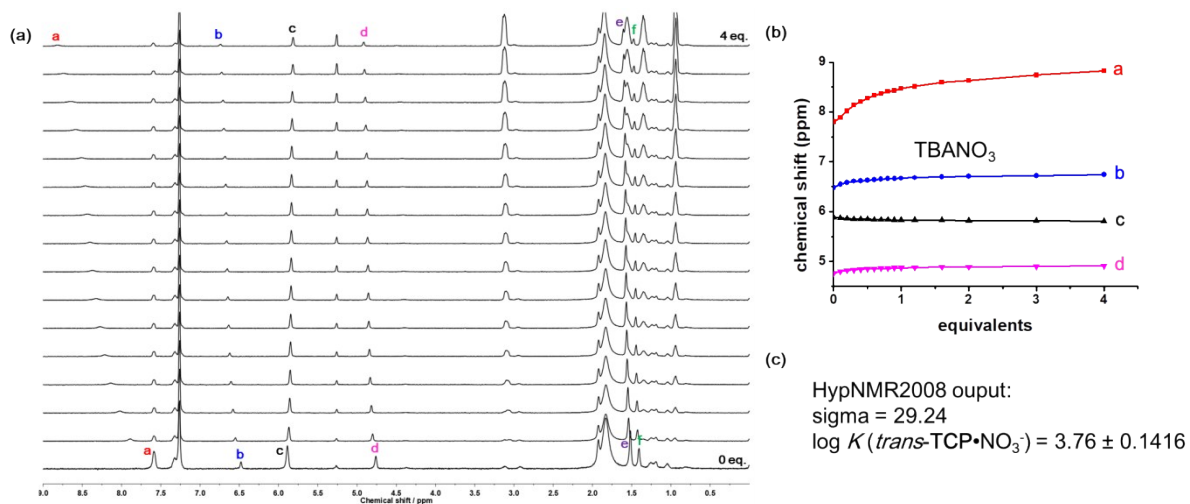


**Figure S11.** (a) Stacked NMR spectra of *trans*-TCP with TBANO<sub>3</sub>, (b) chemical shift change of *trans*-TCP's protons upon addition of TBANO<sub>3</sub>, (c) binding constant calculated from HypNMR.

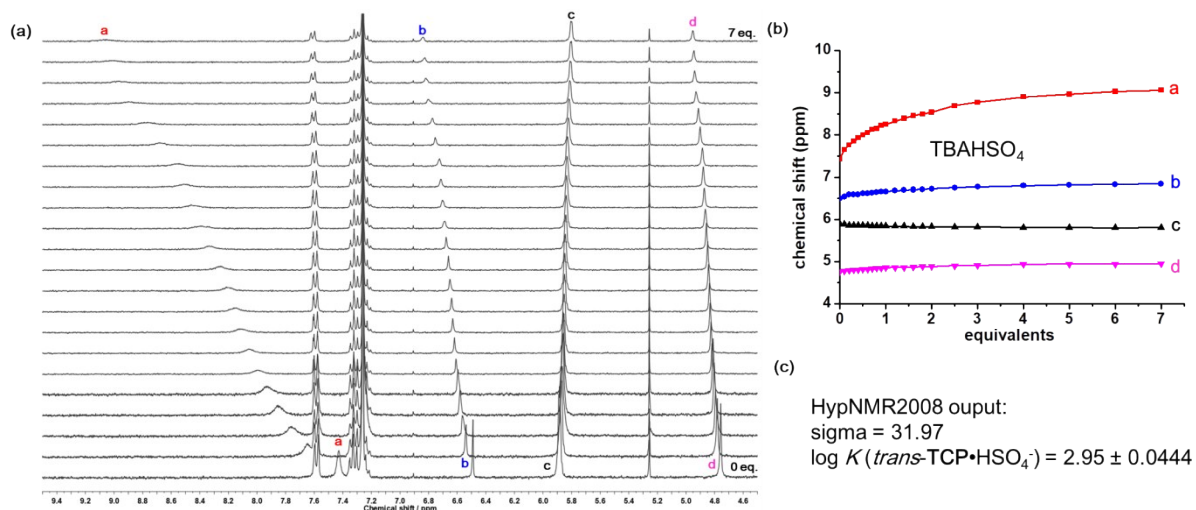


**Figure S12.** (a) Stacked NMR spectra of *trans*-TCP with TBAHSO<sub>4</sub>, (b) chemical shift change of *trans*-TCP's protons upon addition of TBAHSO<sub>4</sub>, (c) binding constant calculated from HypNMR.

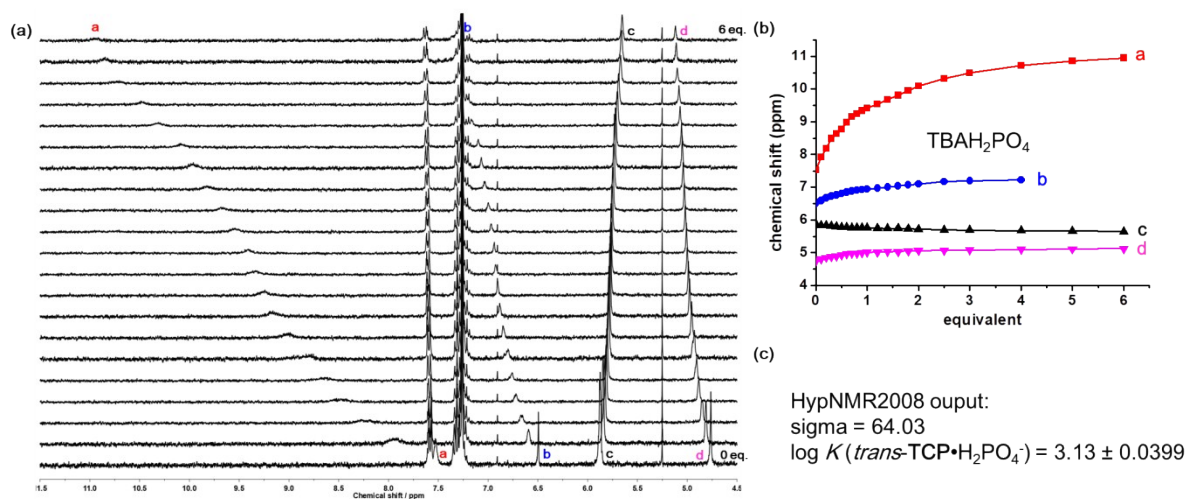


**Figure S13.** (a) Stacked NMR spectra of *trans*-TCP with TBAH<sub>2</sub>PO<sub>4</sub>, (b) chemical shift change of *trans*-TCP's protons upon addition of TBAH<sub>2</sub>PO<sub>4</sub>, (c) binding constant calculated from HypNMR.

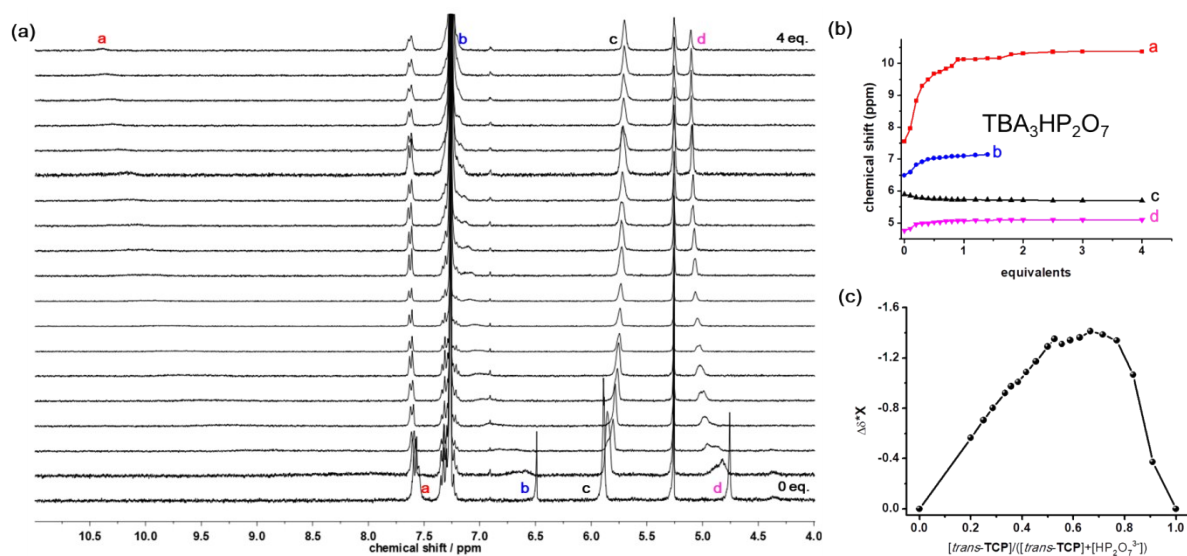


**Figure S14.** (a) Stacked NMR spectra of *trans*-TCP with TBA<sub>3</sub>HP<sub>2</sub>O<sub>7</sub>, (b) chemical shift change of *trans*-TCP's protons upon addition of TBA<sub>3</sub>HP<sub>2</sub>O<sub>7</sub>, (c) Job's plot for the addition of HP<sub>2</sub>O<sub>7</sub><sup>3-</sup> ions to *trans*-TCP.

anion	NO <sub>3</sub> <sup>-</sup>	HSO <sub>4</sub> <sup>-</sup>	H <sub>2</sub> PO <sub>4</sub> <sup>-</sup>
<i>cis</i> -TCP	4.3 × 10 <sup>3</sup>	2.0 × 10 <sup>2</sup>	1.8 × 10 <sup>3</sup>
<i>trans</i> -TCP	5.7 × 10 <sup>3</sup>	8.9 × 10 <sup>2</sup>	1.3 × 10 <sup>3</sup>

**Table S3.** Binding constants ( $K_a$ , M<sup>-1</sup>) of *cis*-TCP, and *trans*-TCP towards various anions in CDCl<sub>3</sub>/CD<sub>3</sub>CN (9/1, v/v) as determined by NMR titration using HypNMR 2008.

## 5. DFT calculation for the optimized structures of TCPs binding with halide ion

All optimized structures of *cis*-TCP and *trans*-TCP binding with halide anions were calculated by using Gaussian 09 program. All structures were optimized at the DFT/WB97XD/6-31G(d) level and CPCM chloroform solvation model. In case of the complexes with iodide were optimized at the DFT/WB97XD/3-21G\* level and CPCM chloroform solvation model.

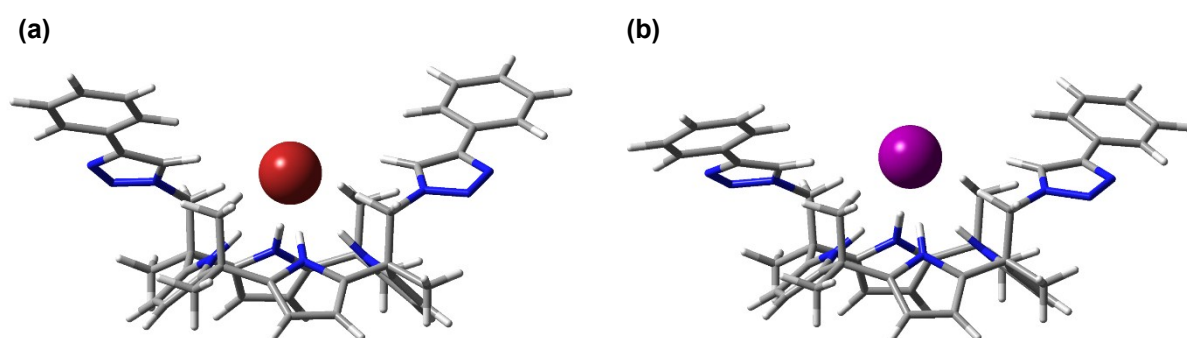


Figure S15. DFT optimized structure of *cis*-TCP with (a) Br<sup>-</sup> and (b) I<sup>-</sup>.

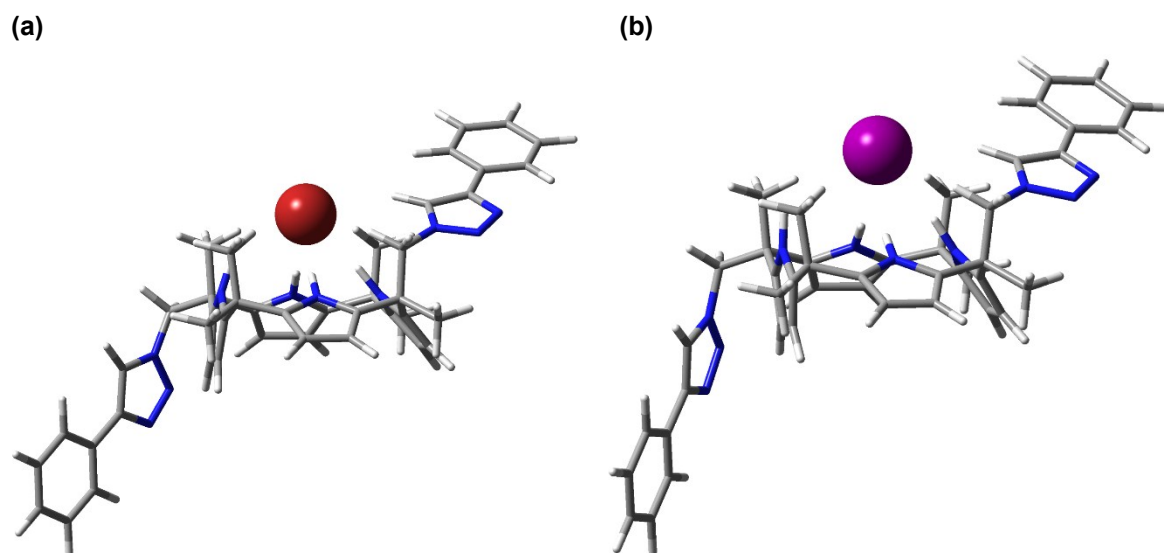


Figure S16. DFT optimized structure of *trans*-TCP with (a) Br<sup>-</sup> and (b) I<sup>-</sup>.

## 6. Reference

1. Á. Martínez-Castañeda, K. Kędziora, I. Lavandera, H. Rodríguez-Solla, C. Concellón and V. del Amo, *Chemical Communications*, 2014, **50**, 2598-2600.
2. A. Arvai and C. Nielsen, *Journal*, 1983.
3. Z. Otwinowski and W. Minor, *Journal*.
4. G. M. Sheldrick, *Acta Crystallographica Section C: Structural Chemistry*, 2015, **71**, 3-8.
5. G. M. Sheldrick, *Acta Crystallographica Section A: Foundations and Advances*, 2015, **71**, 3-8.
6. O. V. Dolomanov, L. J. Bourhis, R. J. Gildea, J. A. Howard and H. Puschmann, *Journal of Applied Crystallography*, 2009, **42**, 339-341.
7. Bruker-AXS. (2007-2013) APEX2 (Ver. 2013.2-0), SADABS (2012-1), and SAINT+ (Ver. 8.30C) Software Reference Manuals. Bruker-AXS, Madison, Wisconsin, USA.
8. G. M. Sheldrick, *Acta Crystallographica Section A: Foundations of Crystallography*, 2008, **64**, 112-122.